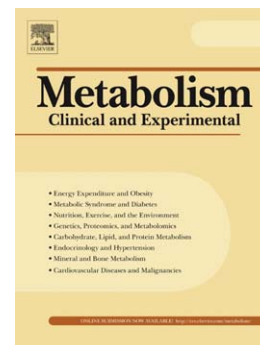# Accepted Manuscript

Effects of hepatic protein tyrosine phosphatase 1B and methionine restriction on hepatic and whole-body glucose and lipid metabolism in mice

E.K. Lees, E. Krol, K. Shearer, N. Mody, T.W. Gettys, M. Delibegović

Please cite this article as: Lees EK, Krol E, Shearer K, Mody N, Gettys TW, Delibegović M, Effects of hepatic protein tyrosine phosphatase 1B and methionine restriction on hepatic and whole-body glucose and lipid metabolism in mice, *Metabolism* (2014), doi: 10.1016/j.metabol.2014.10.038

Effects of hepatic protein tyrosine phosphatase 1B and methionine restriction on hepatic and whole-body glucose and lipid metabolism in mice

E. K. Lees[1], E. Krol[2], K. Shearer[1], N. Mody[1], T. W. Gettys[3] and M. Delibegović[1†].

[1]Institute of Medical Sciences, School of Medical Sciences, University of Aberdeen, Aberdeen, UK. [2]School of Biological Sciences, University of Aberdeen, Aberdeen, UK. [3]Nutrient Sensing and Adipocyte Signaling Department, Pennington Biomedical Research Center, Baton Rouge, LA 70808, USA.

EKL: r01ekl11@abdn.ac.uk, EK: e.krol@abdn.ac.uk, KS: k.d.shearer@abdn.ac.uk, NM: n.mody@abdn.ac.uk, TWG: Thomas.Gettys@pbrc.edu

[†]Corresponding author:

Dr. Mirela Delibegović

Address: Institute of Medical Sciences, School of Medical Sciences, University of Aberdeen, Foresterhill, Aberdeen, AB25 2ZD, UK.

Tel: +44 1224 437587

Fax: +44 1224 437465

Email: m.delibegovic@abdn.ac.uk

Abstract word count: 250

Main text word count: 3600

No. references: 40

No. figures: 5

No. tables: 0

1

Abstract

Aims: Methionine restriction (MR) and hepatic protein tyrosine phosphatase 1B (PTP1B) knockdown both improve hepatic insulin sensitivity by targeting different proteins within the insulin signaling pathway, as well as diminishing hepatic triglyceride content through decreasing hepatic lipogenesis. We hypothesised that a combined approach of hepatic PTP1B inhibition and methionine restriction could lead to a synergistic effect on improvements in glucose homeostasis and lipid metabolism.

Methods: Male and female hepatic-PTP1B knockout (*Alb-Ptp1b*$^{-/-}$) and control wild-type (*Ptp1b*$^{fl/fl}$) mice were maintained on control diet (0.86% methionine) or MR diet (0.172% methionine) for 8 weeks. Body weight and food intake were recorded and physiological tests for whole-body glucose homeostasis were performed. Serum and tissues were analysed biochemically.

Results: MR decreased body weight and increased food intake in *Ptp1b*$^{fl/fl}$ mice as expected, without changing PTP1B protein expression levels or activity. In females, MR treatment alone improved glucose tolerance in *Ptp1b*$^{fl/fl}$ mice, which was further amplified with hepatic-PTP1B deficiency. However, other markers of glucose homeostasis were similar between MR-fed groups. In males, MR improved glucose homeostasis in both, *Alb-Ptp1b*$^{-/-}$ and wild-type *Ptp1b*$^{fl/fl}$ mice to a similar extent. Hepatic-PTP1B inhibition in combination with MR could not further enhance insulin-stimulated hepatic protein kinase B/Akt phosphorylation compared to MR treatment alone and therefore led to no further increase in hepatic insulin signaling. The combined treatment did not further improve lipid metabolism relative to MR diet alone.

Conclusions: Methionine restriction improves glucose and lipid homeostasis; however, adding hepatic PTP1B inhibition to MR is unlikely to yield any additional protective effects.

1. Introduction

Insulin resistance and type 2 diabetes are increasing in prevalence worldwide [1]. Type 2 diabetes is preceded by insulin resistance; characterised by decreased insulin-dependent glucose uptake into peripheral tissues and inadequate suppression of hepatic glucose production, resulting in hyperglycemia [2]. Insulin secretion is initially increased to counteract this; however, type 2 diabetes occurs when the pancreatic beta cells can no longer compensate for the increased demand for insulin

secretion due to loss of beta cell mass [3]. The mechanism(s) behind insulin resistance remain unclear [4, 5] although, it is generally agreed that impaired post-insulin receptor (IR) signal transduction is involved [6].

Insulin signaling is activated when insulin binds to the IR, leading to autophosphorylation of the IR and the ability of it to phosphorylate target substrates including the IRS proteins [6]. Further downstream, protein kinase B (PKB/Akt) is phosphorylated to promote glucose uptake [6]. PKB/Akt also leads to the activation of the mechanistic target of rapamycin complex 1 (mTORC1), which stimulates protein synthesis through activating p70 ribosomal S6 kinase (p70S6K) and its downstream target; ribosomal protein S6 (S6) [6]. Insulin resistance is also linked to the accumulation of hepatic lipids [2], as occurs in non-alcoholic fatty liver disease (NAFLD). NAFLD, which affects 20-35% of the population, is characterised by excess lipid stores within the liver in the absence of alcohol consumption [7].

Methionine restriction (MR) is a dietary modification that involves reducing the amount of the essential amino acid, methionine, to 5-times lower levels than the control diet (0.86% to 0.172%). In comparison to control-fed rodents, MR limits weight gain and diminishes accretion of adiposity, despite increased food intake [8-17] due to stimulation of nonshivering thermogenesis in adipose tissue, leading to elevated energy expenditure [10, 16]. It also improves whole-body glucose homeostasis [8, 11, 12, 17] and insulin signaling in peripheral tissues [11, 17].The enhancement of insulin signaling in the liver by MR is a direct effect of secondarily limiting the availability of the cysteine needed for synthesis of hepatic glutathione (GSH) [17-19]. GSH is an essential co-factor for GSH peroxidase which activates phosphatase and tensin homologue (PTEN) [20] a phosphatase responsible for the dephosphorylation of phosphatidylinositol (3,4,5)-trisphosphate (PIP_3) [6]. The reduction in hepatic glutathione by MR slows the reactivation of PTEN, which increases PIP_3 levels and amplifies downstream PKB/Akt phosphorylation [17]. As MR targets PIP_3, it has no effect on upstream components such as levels of IR or IRS1 phosphorylation [17]. MR also decreases hepatic lipogenesis through targeted effects on lipogenic gene expression, leading to decreased hepatic triglyceride levels [8, 11, 14, 21, 22]. For example, a 16-week MR intervention in human subjects with metabolic syndrome produced a significant reduction in hepatic lipid content [23].

Protein tyrosine phosphatase 1B (PTP1B) is a ubiquitously expressed non-receptor tyrosine phosphatase which negatively regulates leptin and insulin signaling [2, 24-27]. Due to PTP1B downregulating these signaling pathways, whole-body *Ptp1b* knockout mice are lean with enhanced insulin sensitivity [28, 29]. Within the insulin signaling pathway PTP1B directly targets the IR and IRS1 in muscle and liver, whereas it is not a negative regulator of these proteins in adipose tissue [2, 27, 30]. Liver-specific knockout of *Ptp1b* from birth results in improved glucose homeostasis caused by enhanced hepatic insulin signaling [2] and tamoxifen-inducible hepatic *Ptp1b* knockdown in adult

mice leads to the reversal of high-fat diet-induced glucose intolerance [31]. Hepatic PTP1B inhibition also lowers hepatic triacylglycerol storage [31] and lipogenic gene expression [2]. Pharmaceutical companies have been developing PTP1B inhibitors as insulin-sensitizers, and currently the inhibitor trodusquemine is in phase 2 clinical trials [32]. Furthermore, an antisense oligonucleotide targeting PTP1B, developed by ISIS Pharmaceuticals also improved insulin sensitivity in monkeys [33].

Due to hepatic PTP1B directly targeting IR and IRS1 within the insulin signaling pathway and MR acting downstream to amplify PKB/Akt phosphorylation; the aim of this study was to determine if there was a synergistic effect of a dual-therapy on hepatic insulin signaling and whole-body glucose homeostasis.

2. Materials and Methods

2.1. Ethics statement

All animal studies were approved by the University of Aberdeen Ethics Review Board and completed under a project licence (PPL60/3951) approved by the UK Home Office under the Animals (Scientific Procedures) Act 1986.

2.2. Animals

Albumin-Cre mice are crossed with *Ptp1b*fl/fl mice resulting in *Alb-Ptp1b*-/- mice with hepatocyte-specific deletion of PTP1B from birth. *Alb-Ptp1b*-/- and *Ptp1b*fl/fl mice were previously described [2]. Female (5-7 mo old) and male (9-12 mo old) mice studied were on a mixed 129Sv/C57BL6 background. Mice were individually caged and maintained on a 12h-h light/dark cycle at 22-24 °C with free access to food and water. Mice were maintained on a control diet (0.86% methionine) (Dyets, Bethlehem, PA, USA) for 2 weeks. After randomising for body weight, half (females; n=8, males; n=5) of the control *Ptp1b*fl/fl mice were placed on control diet and half (females; n=8, males; n=5) on to MR diet (0.172% methionine) (Dyets, Bethlehem, PA, USA). All *Alb-Ptp1b*-/- mice were placed on MR diet. Glutamic acid content of the MR diet was adjusted to produce equal amounts of total amino acids in both diets. Body weight and food intake were recorded every 3 days. After 8 weeks on the diet, the mice were fasted for 5-hours before being *i.p.* injected with saline or insulin (females 0.8mU/g body weight, males 10mU/g body weight). Cervical dislocation was performed 10 minutes post-injection and tissues were immediately frozen in liquid nitrogen.

2.3. PTP1B activity assay

PTP1B activity was measured as described previously [31]. Briefly, liver lysates were prepared in PTP lysis buffer (130 mmol/l NaCl, 20 mmol/l TRIS (pH 7.5), 5 mmol/l EDTA, 1% Triton X-100 (v/v), 0.5% Nonidet P-40 (v/v)-containing protease inhibitors). PTP1B protein was immunoprecipitated using PTP1B antibody (Millipore, Watford, UK) and protein G-sepharose beads. The reaction was performed using pp60$^{c\text{-}src}$ C-terminal phosphoregulatory peptide (Enzo Life Sciences, Exeter, UK) for 30 minutes at 30°C with constant shaking. The amount of phosphate produced was measured by absorbance at 620 nm and used to indicate level of PTP1B protein activity.

2.4. Immunoblotting

Frozen liver lysates were prepared in RIPA buffer as described previously [27]. Proteins were separated by 4–12% SDS-PAGE and transferred to nitrocellulose membranes. Immunoblots were performed using antibodies from Cell Signaling Technology (Cell Signaling by NEB, Hitchin, UK) (unless stated otherwise) against PTP1B (Millipore, Watford, UK); phospho-S6 (s235/236); total S6; phospho-Akt/PKB (s473); phospho-IR (tyr1163/1163) (Invitrogen, Paisley, UK); IR-β (Santa Cruz, Dallas, TX, USA); total Akt/PKB (Santa Cruz, Dallas, TX, USA) and Glyceraldehyde 3-phosphate dehydrogenase (GAPDH) (Santa Cruz, Dallas, TX, USA). Proteins were visualized using enhanced chemiluminescence and quantified by densitometry scanning (Image J) or Bio-1D software (Peqlab, Sarisbury Green, UK).

2.5. Serum analysis

Six-weeks after beginning MR or control diet, tail vein blood samples were taken following a 5-h fast. All serum measurements were made on these. Serum glucose (glucose oxidase, Thermo Scientific, Waltham, MA, USA) and serum triacylglycerol (Sentinel Diagnostics, Milan, Italy) were measured using appropriate kits. Serum insulin and leptin (CrystalChem, Downers Grove, IL, USA) were determined by ELISA. Serum NEFAs were measured using a kit (Wako Chemicals, Richmond, VA, USA). Assays were measured using a Spectramax Plus 384 spectrophotometer (Molecular Devices, Sunnyvale, CA, USA).

2.6. Glucose and pyruvate tolerance tests

Glucose tolerance tests were performed after 5-weeks of dietary treatment. Mice were *i.p*. injected, following a 5-h fast, with 2 mg/g BW glucose. For pyruvate tolerance tests, performed after 7-weeks of dietary treatment, mice were injected with 2 mg/g pyruvate. Tail blood glucose measurements using glucometers (AlphaTRAK, Berkshire, UK) were taken immediately before and at 15, 30, 60 and 120 min post-injection.

2.7. Gene expression analysis

Total RNA was isolated from mouse liver using peqGOLD TriFast (Peqlab, Sarisbury Green, UK). First strand cDNA was synthesized from 1 μg of total RNA using bioscript cDNA synthesis kit (Bioline, London, UK), oligo (dT) 18 primers and random hexamer primers. Quantitative PCR (qPCR) was used to amplify target genes using GoTaq qPCR Master Mix (Promega, Southampton, UK) and gene-specific primers on the Roche LightCycler® 480 System (Roche Diagnostics, Burgess Hill, UK). Relative gene expression was calculated using the Pfaffl method [34] and normalised to the reference gene hypoxanthine-guanine phosphoribosyltransferase (*Hprt*).

2.8. Data analysis

 Data are expressed as mean ± SEM. Statistical analyses were performed using repeated measures two-way ANOVA with Bonferroni multiple comparison post-tests or one-way ANOVA with Tukey's multiple comparison post-tests, as appropriate. $P < 0.05$ was considered statistically significant. GraphPad Prism 5 statistical software (GraphPad Software, Inc., San Diego, CA, USA) was used for analyses.

3. Results

3.1. MR does not affect hepatic PTP1B protein or activity levels

To be able to assess if any further improvements in glucose or lipid homeostasis occur when adding hepatic PTP1B inhibition to MR, it was first important to ensure that MR was not affecting hepatic PTP1B or activity levels. Hepatic PTP1B protein levels were significantly decreased by 32% in female MR-fed *Alb-Ptp1b*^{-/-} mice relative to female MR-fed *Ptp1b*^{fl/fl} mice (Fig. 1A and B). Hepatic PTP1B protein activity was also decreased by 40% in female MR-fed *Alb-Ptp1b*^{-/-} mice compared to

female MR-fed $Ptp1b^{fl/fl}$ mice (Fig. 1C). MR diet in $Ptp1b^{fl/fl}$ female mice had no effect on hepatic PTP1B protein or activity levels, compared to control-fed $Ptp1b^{fl/fl}$ mice (Fig. 1A, B and C).

3.2. MR decreases body weight in both Alb-Ptp1b$^{-/-}$ and Ptp1b$^{fl/fl}$ mice.

Both female and male mice on MR ($Ptp1b^{fl/fl}$ and $Alb\text{-}Ptp1b^{-/-}$) exhibited decreased body weight throughout the course of the study compared to control-fed $Ptp1b^{fl/fl}$ mice (Fig. 2A and B). Female MR-fed $Ptp1b^{fl/fl}$ and MR-fed $Alb\text{-}Ptp1b^{-/-}$ mice had significantly lower body weight relative to control-fed $Ptp1b^{fl/fl}$ mice from days 22-43 of the dietary treatment (Fig. 2A). MR-fed $Ptp1b^{fl/fl}$ and MR-fed $Alb\text{-}Ptp1b^{-/-}$ mice did not differ in body weight levels throughout the duration of the study in both female and male mice (Fig. 2A and B). Food intake (g/ g BW/ day) was significantly increased in female and male MR-fed $Alb\text{-}Ptp1b^{-/-}$ mice and also elevated in MR-fed $Ptp1b^{fl/fl}$ mice compared to control-fed $Ptp1b^{fl/fl}$ mice (Fig. 2C and D) There were no differences in food intake in either female or male groups between MR-fed $Ptp1b^{fl/fl}$ and MR-fed $Alb\text{-}Ptp1b^{-/-}$ mice (Fig. 2C and D).

3.3. MR and hepatic PTP1B knockdown increase hepatic insulin signaling but do not act synergistically.

MR alone had no effect on levels of phosphorylation of the IR (MR-fed $Ptp1b^{fl/fl}$ vs. control-fed $Ptp1b^{fl/fl}$ mice) (Fig. 3A and C). MR-fed $Alb\text{-}Ptp1b^{-/-}$ mice did increase levels of phosphorylation of the IR compared to both MR-fed $Ptp1b^{fl/fl}$ and control-fed $Ptp1b^{fl/fl}$ mice (Fig. 3A and C). Both groups on MR ($Ptp1b^{fl/fl}$ and $Alb\text{-}Ptp1b^{-/-}$) had increased levels of phosphorylation of PKB/Akt and an increased ratio of phosphorylated to total PKB/Akt relative to control-fed $Ptp1b^{fl/fl}$ mice (Fig. 3A, B and D). The two groups fed MR diet ($Ptp1b^{fl/fl}$ and $Alb\text{-}Ptp1b^{-/-}$) did not differ from each other in levels of phosphorylation of PKB/Akt or ratio of phosphorylated to total PKB/Akt (Fig. 3A, B and D). There were no differences for diet or genotype on levels of phosphorylated or total S6 (Fig. 3A, B and E).

3.4. Hepatic PTP1B knockdown does not further improve glucose homeostasis except in levels of glucose tolerance in females.

In female mice, MR significantly increased glucose tolerance in $Ptp1b^{fl/fl}$ mice relative to control-fed $Ptp1b^{fl/fl}$ mice (Fig. 4A). Female MR-fed $Alb\text{-}Ptp1b^{-/-}$ mice improved glucose tolerance even further and significantly enhanced glucose tolerance compared to control-fed $Ptp1b^{fl/fl}$ mice and MR-fed $Ptp1b^{fl/fl}$ mice (Fig. 4A). In males, MR-fed $Ptp1b^{fl/fl}$ mice had an improved response to a glucose

challenge compared to control-fed $Ptp1b^{fl/fl}$ mice. MR-fed $Alb\text{-}Ptp1b^{-/-}$ mice significantly enhanced glucose tolerance compared to control-fed $Ptp1b^{fl/fl}$ mice; however, there was no additional improvement in glucose tolerance between MR-fed $Ptp1b^{fl/fl}$ and MR-fed $Alb\text{-}Ptp1b^{-/-}$ mice (Fig. 4B). To examine if there was any additional effect of supplementing MR with hepatic PTP1B knockdown on suppression of hepatic gluconeogenesis, we performed a pyruvate-tolerance test (PTT) in female mice (Fig. 4C). MR-fed $Alb\text{-}Ptp1b^{-/-}$ mice significantly improved and MR-fed $Ptp1b^{fl/fl}$ mice also enhanced their response to a pyruvate challenge compared to control-fed $Ptp1b^{fl/fl}$ mice; however, there were no additional differences between MR-fed $Ptp1b^{fl/fl}$ and MR-fed $Alb\text{-}Ptp1b^{-/-}$ mice (Fig. 4C). Both MR-fed $Ptp1b^{fl/fl}$ and MR-fed $Alb\text{-}Ptp1b^{-/-}$ female mice had significantly decreased fasting blood glucose levels relative to control-fed $Ptp1b^{fl/fl}$ mice (Fig. 4D). There were no additive differences between MR-fed $Ptp1b^{fl/fl}$ and MR-fed $Alb\text{-}Ptp1b^{-/-}$ mice in fasting blood glucose levels (Fig. 4D). In male mice, there were no differences between groups on fasting blood glucose levels (Fig. 4E). In both female and male mice both groups fed MR ($Ptp1b^{fl/fl}$ and $Alb\text{-}Ptp1b^{-/-}$) showed significantly lower fasting serum insulin levels relative to control-fed $Ptp1b^{fl/fl}$ mice (Fig. 4F and G). Again, there was no difference between MR-fed $Ptp1b^{fl/fl}$ and MR-fed $Alb\text{-}Ptp1b^{-/-}$ mice for fasting serum insulin levels in either female or male mice (Fig. 4F and G).

3.5. MR improves lipid homeostasis which is not further exacerbated by hepatic PTP1B knockdown

Both MR-fed $Ptp1b^{fl/fl}$ and MR-fed $Alb\text{-}Ptp1b^{-/-}$ female mice had significantly decreased fasting serum leptin levels relative to control-fed $Ptp1b^{fl/fl}$ mice (Fig. 5A). However, there were no additional differences between MR-fed $Ptp1b^{fl/fl}$ and MR-fed $Alb\text{-}Ptp1b^{-/-}$ mice in fasting serum leptin levels in female mice (Fig. 5A). In male mice, both MR-fed $Ptp1b^{fl/fl}$ and MR-fed $Alb\text{-}Ptp1b^{-/-}$ mice had lower fasting serum leptin levels compared to control-fed $Ptp1b^{fl/fl}$ mice; yet again these were not additive (Fig. 5B). Diet and genotype had no effect on fasting serum NEFA levels or fasting serum triacylglycerol levels in either female or male mice (Fig. 5C, D, E and F). In female mice, both MR-fed $Ptp1b^{fl/fl}$ and MR-fed $Alb\text{-}Ptp1b^{-/-}$ mice had significantly decreased hepatic gene expression of $Srebp1c$ and also decreased expression of other lipogenic genes, including $Srebp1a$ and Fas relative to control-fed $Ptp1b^{fl/fl}$ mice (Fig. 5G). There were no differences in levels of these hepatic lipogenic genes between MR-fed $Ptp1b^{fl/fl}$ and MR-fed $Alb\text{-}Ptp1b^{-/-}$ female mice (Fig. 5G). Both female MR-fed $Ptp1b^{fl/fl}$ and MR-fed $Alb\text{-}Ptp1b^{-/-}$ mice showed reduced hepatic gluconeogenesis through decreased mRNA expression of G$lucose\text{-}6\text{-}phosphate$ ($G6p$) relative to control-fed $Ptp1b^{fl/fl}$ mice, but the two MR-fed groups ($Ptp1b^{fl/fl}$ and $Alb\text{-}Ptp1b^{-/-}$) did not differ from each other (Fig. 5G).

4. Discussion

The increasing prevalence of metabolic syndrome demands more effective drug therapies [35]. MR produces many beneficial effects including reduced body mass and adiposity and improved glucose homeostasis [8-17]. We have shown previously that both hepatic PTP1B deletion from birth or knockdown in adult insulin-resistance mice protects against the development of insulin resistance and reverses established glucose intolerance, respectively [2, 31, 36]. These studies established definitively that in the liver, PTP1B deletion results in increased IR and IRS1 phosphorylation. Recent studies on the beneficial insulin sensitizing effects of MR diet in the liver revealed that hepatic PKB/Akt phosphorylation is enhanced [11, 17]. We therefore hypothesised that there could be an additive effect on hepatic insulin sensitivity and whole-body glucose homeostasis if MR diet is combined with liver PTP1B deficiency. Our study suggests that MR improves glucose homeostasis and lipid metabolism; however, there were no major additional therapeutic effects of the combined treatment.

Hepatic PTP1B protein levels and PTP1B enzyme activity levels in female mice were decreased as expected in the *Alb-Ptp1b*$^{-/-}$ mice. The MR-fed *Alb-Ptp1b*$^{-/-}$ mice did not present a complete deletion of PTP1B within the liver as it has in other studies [2], but rather a 32% decrease in protein and 40% decrease in activity levels; however, the deletion is hepatocyte-specific and so there are other cell types expressing normal levels of PTP1B within the whole liver lysates used for these assays [2]. The level of deletion would be consistent with the physiological level of PTP1B inhibition expected to be achieved by inhibitor drugs and therefore the results represent applicable findings [37]. It was recently reported that MR limits the activity of hepatic phosphatase PTEN, and the authors found no evidence to suggest that PTP1B was a target of the diet [17]. Thus, it is important that we found that MR itself had no effect on hepatic levels of PTP1B protein or activity so that we could directly assess the utility of a combined treatment.

MR causes a decrease in body weight despite elevating food intake [8-17]; however, hepatic PTP1B deletion has no affect on energy balance [2, 31]. The body weight loss and increased food intake produced by MR compared to control-fed mice was similar between genotypes and is therefore likely to be an effect of MR only. The study also found that MR can decrease body weight and enhance energy intake in mice on a new genetic background (129Sv/C57BL6), confirming findings from other genetic backgrounds [8, 11, 13, 16, 17].

In agreement with previous findings, which demonstrated that hepatic PTP1B directly targets the IR and IRS1 [2], *Alb-Ptp1b*$^{-/-}$ mice had increased levels of phosphorylation of the IR compared to *Ptp1b*$^{fl/fl}$ mice. MR itself caused no change in phosphorylation levels of hepatic IR, consistent with recent findings which demonstrated that MR limits degradation of PIP$_3$, leading to enhanced downstream activation and phosphorylation of PKB/Akt, which we also found in this study [17]. It

was hypothesised that hepatic PTP1B inhibition in combination with MR would act additionally on phosphorylation of PKB/Akt; however, this was similar between the combined treatment and MR alone. It may be that MR-treatment alone already leads to maximally increased PKB/Akt phosphorylation so that increased signaling upstream of PKB/Akt at the level of IR/IRS1 (achieved by PTP1B inhibition) cannot lead to further improvements. This may suggest that this is the major mode of action that MR plays in the liver.

Consistent with MR's known effects to improve glucose homeostasis, MR in both groups improved glucose tolerance and lowered blood glucose and serum insulin levels compared to control-fed *Ptp1b*$^{fl/fl}$ mice [8, 9, 11, 12, 17]. This was further improved by PTP1B knockdown in a glucose tolerance test in female mice; however, there was no additional effect present in the male mice. The reason behind the additional improvements in glucose tolerance in female mice that were not present in male mice could be due to the male mice being older and therefore naturally more glucose intolerant compared to the females [38]. Furthermore, we cannot exclude the possibility that sex hormones such as estrogen play an additional beneficial and protective role in the MR-fed *Alb-Ptp1b*$^{-/-}$ mice [39]. Blood glucose levels in a pyruvate tolerance test and fasting blood glucose and serum insulin levels were similarly lowered between female MR-fed *Ptp1b*$^{fl/fl}$ and MR-fed *Alb-Ptp1b*$^{-/-}$ mice. There was also no further improvement by inhibition of hepatic-PTP1B in the male mice. Since the combined-treatment of MR and hepatic PTP1B inhibition did not result in additional enhancement in hepatic insulin signaling, or suppression of blood glucose, serum insulin and hepatic gluconeogenic genes, this suggests that MR alone is sufficient to observe these beneficial effects.

Interestingly, the combined MR and hepatic PTP1B inhibition treatment produced no further improvements in lipid metabolism to MR alone, with fasting serum leptin levels being the same between the MR-fed groups, but both lower than *Ptp1b*$^{fl/fl}$ control-fed mice. Due to no additional effect of hepatic PTP1B knockdown this finding is most likely due to MR decreasing adiposity levels [8-12, 14-16]. MR decreases hepatic lipogenesis [9-11, 14, 21, 40] and hepatic PTP1B deletion has also been shown to produce similar findings [2]; but again, supplementing MR with hepatic PTP1B inhibition led to no further effects on hepatic lipogenesis. This could be due to MR inhibiting lipogenic gene expression by such a substantial amount that hepatic PTP1B inhibition cannot decrease gene expression further, or it is possible that there is a common mechanism behind these two treatments. Both MR-fed groups expressed decreased hepatic gluconeogenesis compared to control-fed *Ptp1b*$^{fl/fl}$ mice, although adding hepatic PTP1B inhibition to MR led to no further reduction. This corresponds with the same level of insulin-stimulated PKB/Akt activation in both MR-fed groups, as gluconeogenesis is down-regulated downstream of PKB/Akt [6]. MR was shown in a recent study to inhibit hepatic gluconeogenesis [11] and hepatic PTP1B knockdown also decreases hepatic gluconeogenic gene expression [2, 31].

In conclusion, although MR and hepatic PTP1B inhibition have separate targets in the insulin signaling pathway, our findings suggest that when their effects downstream converge on PKB/Akt, the signal is not further amplified.

Conflicts of interest

The authors declare that there is no duality of interest associated with this manuscript.

Contribution statement

EKL, EK and KS contributed to acquisition of data. EKL, NM, TWG and MD contributed to design, analysis and interpretation of data. EKL wrote the first draft of the manuscript and EK, KS, NM, TWG and MD contributed to the critical revision of the manuscript. All authors approved the final version of the manuscript.

References

1 Zimmet P, Alberti KG, Shaw J. Global and societal implications of the diabetes epidemic. *Nature* 2001;414(6865):782-7.

2 Delibegovic M, Zimmer D, Kauffman C, et al. Liver-specific deletion of protein-tyrosine phosphatase 1B (PTP1B) improves metabolic syndrome and attenuates diet-induced endoplasmic reticulum stress. *Diabetes* 2009;58(3):590-9.

3 Rhodes CJ. Type 2 diabetes-a matter of beta-cell life and death? *Science* 2005;307(5708):380-4.

4 Kobayashi K. Adipokines: therapeutic targets for metabolic syndrome. *Curr Drug Targets* 2005;6(4):525-9.

5 Shulman GI. Cellular mechanisms of insulin resistance. *J Clin Invest* 2000;106(2):171-6.

6 Taniguchi CM, Emanuelli B, Kahn CR. Critical nodes in signaling pathways: insights into insulin action. *Nat Rev Mol Cell Biol* 2006;7(2):85-96.

7 Moore JB. Non-alcoholic fatty liver disease: the hepatic consequence of obesity and the metabolic syndrome. *Proc Nutr Soc* 2010;69(2):211-20.

8 Ables GP, Perrone CE, Orentreich D, et al. Methionine-restricted C57BL/6J mice are resistant to diet-induced obesity and insulin resistance but have low bone density. *PLoS One* 2012;7(12):e51357.

9 Anthony TG, Morrison CD, Gettys TW. Remodeling of lipid metabolism by dietary restriction of essential amino acids. *Diabetes* 2013;62(8):2635-44.

10 Hasek BE, Stewart LK, Henagan TM, et al. Dietary methionine restriction enhances metabolic flexibility and increases uncoupled respiration in both fed and fasted states. *Am J Physiol Regul Integr Comp Physiol* 2010;299(3):R728-39.

11 Lees EK, Krol E, Grant L, et al. Methionine restriction restores a younger metabolic phenotype in adult mice with alterations in fibroblast growth factor 21. *Aging Cell* 2014;.

12 Malloy VL, Krajcik RA, Bailey SJ, et al. Methionine restriction decreases visceral fat mass and preserves insulin action in aging male Fischer 344 rats independent of energy restriction. *Aging Cell* 2006;5(4):305-14.

13 Miller RA, Buehner G, Chang Y, et al. Methionine-deficient diet extends mouse lifespan, slows immune and lens aging, alters glucose, T4, IGF-I and insulin levels, and increases hepatocyte MIF levels and stress resistance. *Aging Cell* 2005;4(3):119-25.

14 Perrone CE, Mattocks DA, Jarvis-Morar M, et al. Methionine restriction effects on mitochondrial biogenesis and aerobic capacity in white adipose tissue, liver, and skeletal muscle of F344 rats. *Metabolism* 2010;59(7):1000-11.

15 Perrone CE, Malloy VL, Orentreich DS, et al. Metabolic adaptations to methionine restriction that benefit health and lifespan in rodents. *Exp Gerontol* 2013;48(7):654-60.

16 Plaisance EP, Henagan TM, Echlin H, et al. Role of beta-adrenergic receptors in the hyperphagic and hypermetabolic responses to dietary methionine restriction. *Am J Physiol Regul Integr Comp Physiol* 2010;299(3):R740-50.

17 Stone KP, Wanders D, Orgeron M, et al. Mechanisms of Increased in Vivo Insulin Sensitivity by Dietary Methionine Restriction in Mice. *Diabetes* 2014;.

18 Richie JP,Jr, Leutzinger Y, Parthasarathy S, et al. Methionine restriction increases blood glutathione and longevity in F344 rats. *FASEB J* 1994;8(15):1302-7.

19 Richie JP,Jr, Komninou D, Leutzinger Y, et al. Tissue glutathione and cysteine levels in methionine-restricted rats. *Nutrition* 2004;20(9):800-5.

20 Kim Y, Song YB, Kim TY, et al. Redox regulation of the tumor suppressor PTEN by glutathione. *FEBS Lett* 2010;584(16):3550-6.

21 Hasek BE, Boudreau A, Shin J, et al. Remodeling the integration of lipid metabolism between liver and adipose tissue by dietary methionine restriction in rats. *Diabetes* 2013;62(10):3362-72.

22 Malloy VL, Perrone CE, Mattocks DA, et al. Methionine restriction prevents the progression of hepatic steatosis in leptin-deficient obese mice. *Metabolism* 2013;62(11):1651-61.

23 Plaisance EP, Greenway FL, Boudreau A, et al. Dietary methionine restriction increases fat oxidation in obese adults with metabolic syndrome. *J Clin Endocrinol Metab* 2011;96(5):E836-40.

24 Bence KK, Delibegovic M, Xue B, et al. Neuronal PTP1B regulates body weight, adiposity and leptin action. *Nat Med* 2006;12(8):917-24.

25 Tsou RC, Zimmer DJ, De Jonghe BC, et al. Deficiency of PTP1B in leptin receptor-expressing neurons leads to decreased body weight and adiposity in mice. *Endocrinology* 2012;153(9):4227-37.

26 Yip SC, Saha S, Chernoff J. PTP1B: a double agent in metabolism and oncogenesis. *Trends Biochem Sci* 2010;35(8):442-9.

27 Delibegovic M, Bence KK, Mody N, et al. Improved glucose homeostasis in mice with muscle-specific deletion of protein-tyrosine phosphatase 1B. *Mol Cell Biol* 2007;27(21):7727-34.

28 Elchebly M, Payette P, Michaliszyn E, et al. Increased insulin sensitivity and obesity resistance in mice lacking the protein tyrosine phosphatase-1B gene. *Science* 1999;283(5407):1544-8.

29 Klaman LD, Boss O, Peroni OD, et al. Increased energy expenditure, decreased adiposity, and tissue-specific insulin sensitivity in protein-tyrosine phosphatase 1B-deficient mice. *Mol Cell Biol* 2000;20(15):5479-89.

30 Owen C, Czopek A, Agouni A, et al. Adipocyte-specific protein tyrosine phosphatase 1B deletion increases lipogenesis, adipocyte cell size and is a minor regulator of glucose homeostasis. *PLoS One* 2012;7(2):e32700.

31 Owen C, Lees EK, Grant L, et al. Inducible liver-specific knockdown of protein tyrosine phosphatase 1B improves glucose and lipid homeostasis in adult mice. *Diabetologia* 2013;56(10):2286-96.

32 Lantz KA, Hart SG, Planey SL, et al. Inhibition of PTP1B by trodusquemine (MSI-1436) causes fat-specific weight loss in diet-induced obese mice. *Obesity (Silver Spring)* 2010;18(8):1516-23.

33 Swarbrick MM, Havel PJ, Levin AA, et al. Inhibition of protein tyrosine phosphatase-1B with antisense oligonucleotides improves insulin sensitivity and increases adiponectin concentrations in monkeys. *Endocrinology* 2009;150(4):1670-9.

34 Pfaffl MW. A new mathematical model for relative quantification in real-time RT-PCR. *Nucleic Acids Res* 2001;29(9):e45.

35 Ford ES, Giles WH, Mokdad AH. Increasing prevalence of the metabolic syndrome among u.s. Adults. *Diabetes Care* 2004;27(10):2444-9.

36 Agouni A, Mody N, Owen C, et al. Liver-specific deletion of protein tyrosine phosphatase (PTP) 1B improves obesity- and pharmacologically induced endoplasmic reticulum stress. *Biochem J* 2011;438(2):369-78.

37 Zinker BA, Rondinone CM, Trevillyan JM, et al. PTP1B antisense oligonucleotide lowers PTP1B protein, normalizes blood glucose, and improves insulin sensitivity in diabetic mice. *Proc Natl Acad Sci U S A* 2002;99(17):11357-62. 38 Selman C, Withers, DJ. Mammalian models of extended healthy lifespan. *Philos. Trans. R. Soc. Lond. B Biol. Sci.*2011;366(1561):99-107.

39 Foryst-Ludwig A, Kintscher U. Metabolic impact of estrogen signalling through ERalpha and ERbeta. *J Steroid Biochem Mol Biol*. 2010;122(1-3):74-81.

40 Perrone CE, Mattocks DA, Plummer JD, et al. Genomic and metabolic responses to methionine-restricted and methionine-restricted, cysteine-supplemented diets in Fischer 344 rat inguinal adipose tissue, liver and quadriceps muscle. *J Nutrigenet Nutrigenomics* 2012;5(3):132-57.

Figure legends

Fig. 1 Hepatic PTP1B protein and activity levels in female mice. (a) Hepatic PTP1B protein levels of CON *Ptp1b*$^{fl/fl}$ mice (n=4), MR *Ptp1b*$^{fl/fl}$ (n=4) and MR *Alb-Ptp1b*$^{-/-}$ (n=4). (b) Quantification of hepatic PTP1B protein levels in CON *Ptp1b*$^{fl/fl}$ mice (n=7), MR *Ptp1b*$^{fl/fl}$ (n=8) and MR *Alb-Ptp1b*$^{-/-}$ (n=8). (c) Hepatic PTP1B activity levels in CON *Ptp1b*$^{fl/fl}$ mice (n=5), MR *Ptp1b*$^{fl/fl}$ (n=6) and MR *Alb-Ptp1b*$^{-/-}$ (n=5). Data are represented as mean ± s.e.m. White bars, CON *Ptp1b*$^{fl/fl}$; grey bars, MR *Ptp1b*$^{fl/fl}$;black bars, MR *Alb-Ptp1b*$^{-/-}$. Data were analysed by one-way ANOVA with Tukey's multiple comparison post hoc test. \$ MR *Alb-Ptp1b*$^{-/-}$ mice significantly different to MR *Ptp1b*$^{fl/fl}$ mice ($p<0.05$). # MR *Alb-Ptp1b*$^{-/-}$ mice significantly different to CON *Ptp1b*$^{fl/fl}$ mice ($p<0.05$).

Fig. 2 Body weight and food intake. (a) Body weight of female CON *Ptp1b*$^{fl/fl}$ (n=8), MR *Ptp1b*$^{fl/fl}$ (n=8) and MR *Alb-Ptp1b*$^{-/-}$ mice (n=8). (b) Body weight of male CON *Ptp1b*$^{fl/fl}$ (n=5), MR *Ptp1b*$^{fl/fl}$ (n=5) and MR *Alb-Ptp1b*$^{-/-}$ mice (n=5). (c) Food intake of female CON *Ptp1b*$^{fl/fl}$ (n=5), MR *Ptp1b*$^{fl/fl}$ (n=4) and MR *Alb-Ptp1b*$^{-/-}$ mice (n=7). (d) Food intake of male CON *Ptp1b*$^{fl/fl}$ (n=5), MR *Ptp1b*$^{fl/fl}$ (n=4) and MR *Alb-Ptp1b*$^{-/-}$ mice (n=5). Data are represented as mean ± s.e.m. White circles, CON *Ptp1b*$^{fl/fl}$; grey squares, MR *Ptp1b*$^{fl/fl}$; black triangles, MR *Alb-Ptp1b*$^{-/-}$. Data were analysed by repeated measures two-way ANOVA with Bonferroni multiple comparison post hoc tests.* MR *Alb-Ptp1b*$^{-/-}$ and MR *Ptp1b*$^{fl/fl}$ mice significantly different to CON *Ptp1b*$^{fl/fl}$ mice ($p<0.05$). & MR *Ptp1b*$^{fl/fl}$ mice significantly different to CON *Ptp1b*$^{fl/fl}$ mice ($p<0.05$). # MR *Alb-Ptp1b*$^{-/-}$ mice significantly different to CON *Ptp1b*$^{fl/fl}$ mice ($p<0.05$).

Fig. 3 Hepatic insulin signaling in male mice. (a) Immunoblots of pIR (tyr 1162/1163), pAKT/PKB (Ser 473) and pS6 (ser 235/236) in insulin-stimulated CON *Ptp1b*$^{fl/fl}$ (n=5), MR *Ptp1b*$^{fl/fl}$ (n=5) and

MR $Alb\text{-}Ptp1b^{-/-}$ mice (n=5). (b) Immunoblots of IR-β, Akt and S6 in insulin-stimulated CON $Ptp1b^{fl/fl}$ (n=5), MR $Ptp1b^{fl/fl}$ (n=5) and MR $Alb\text{-}Ptp1b^{-/-}$ mice (n=5). (c) Quantification of pIR, IR- β and pIR/IR-β in CON $Ptp1b^{fl/fl}$ (n=5), MR $Ptp1b^{fl/fl}$ (n=5) and MR $Alb\text{-}Ptp1b^{-/-}$ mice (n=5). (d) Quantification of pAkt, Akt and pAkt/Akt in CON $Ptp1b^{fl/fl}$ (n=5), MR $Ptp1b^{fl/fl}$ (n=5) and MR $Alb\text{-}Ptp1b^{-/-}$ mice (n=5). (e) Quantification of pS6, S6 and pS6/S6 in CON $Ptp1b^{fl/f}$ (n=5), MR $Ptp1b^{fl/fl}$ (n=5) and MR $Alb\text{-}Ptp1b^{-/-}$ mice (n=5). Phosphorylated proteins and total proteins were each normalised to ponceau and then ratio of phosphorylated:total calculated. S = i.p. injected with saline as control. Data are represented as mean ± s.e.m. White bars, CON $Ptp1b^{fl/fl}$; grey bars, MR $Ptp1b^{fl/fl}$; black bars, MR $Alb\text{-}Ptp1b^{-/-}$. Data were analysed by one-way ANOVA with Tukey's multiple comparison post hoc test.

Fig. 4 Glucose homeostasis. Glucose tolerance assessed by a GTT after a 5-h fast was performed on (a) female CON $Ptp1b^{fl/fl}$ (n=8), MR $Ptp1b^{fl/fl}$ (n=8) and MR $Alb\text{-}Ptp1b^{-/-}$ mice (n=8) and (b) male CON $Ptp1b^{fl/fl}$ (n=5), MR $Ptp1b^{fl/fl}$ (n=5) and MR $Alb\text{-}Ptp1b^{-/-}$ mice (n=5). (c) Pyruvate tolerance assessed by a PTT after a 5-h fast was performed on female CON $Ptp1b^{fl/fl}$ (n=8), MR $Ptp1b^{fl/fl}$ (n=8) and MR $Alb\text{-}Ptp1b^{-/-}$ mice (n=8). Fasting blood glucose levels were measured in (d) female CON $Ptp1b^{fl/fl}$ (n=8), MR $Ptp1b^{fl/fl}$ (n=8) and MR $Alb\text{-}Ptp1b^{-/-}$ mice (n=8) and (e) male CON $Ptp1b^{fl/fl}$ (n=5), MR $Ptp1b^{fl/fl}$ (n=5) and MR $Alb\text{-}Ptp1b^{-/-}$ mice (n=5). Fasting serum insulin levels were measured in (f) female CON $Ptp1b^{fl/fl}$ (n=8), MR $Ptp1b^{fl/fl}$ (n=8) and MR $Alb\text{-}Ptp1b^{-/-}$ mice (n=8) and (g) male CON $Ptp1b^{fl/fl}$ (n=5), MR $Ptp1b^{fl/fl}$ (n=5) and MR $Alb\text{-}Ptp1b^{-/-}$ mice (n=5). Data are represented as mean ± s.e.m. White circles/bars, CON $Ptp1b^{fl/fl}$; grey squares/bars, MR $Ptp1b^{fl/fl}$; black triangles/bars, MR $Alb\text{-}Ptp1b^{-/-}$. Data were analysed by repeated measures two-way ANOVA with Bonferroni multiple comparison post hoc tests or one-way ANOVA with Tukey's multiple comparison post hoc test.* MR $Alb\text{-}Ptp1b^{-/-}$ and MR $Ptp1b^{fl/fl}$ mice significantly different to CON $Ptp1b^{fl/fl}$ mice (p<0.05). \$ MR $Alb\text{-}Ptp1b^{-/-}$ mice significantly different to MR $Ptp1b^{fl/fl}$ mice (p<0.05). # MR $Alb\text{-}Ptp1b^{-/-}$ mice significantly different to CON $Ptp1b^{fl/fl}$ mice (p<0.05).

Fig. 5 Lipid homeostasis. Fasting serum leptin levels were measured in (a) female CON $Ptp1b^{fl/fl}$ (n=8), MR $Ptp1b^{fl/fl}$ (n=8) and MR $Alb\text{-}Ptp1b^{-/-}$ mice (n=8) and (b) male CON $Ptp1b^{fl/fl}$ (n=4), MR $Ptp1b^{fl/fl}$ (n=4) and MR $Alb\text{-}Ptp1b^{-/-}$ mice (n=5). Fasting serum NEFA levels were measured in (c) female CON $Ptp1b^{fl/fl}$ (n=8), MR $Ptp1b^{fl/fl}$ (n=8) and MR $Alb\text{-}Ptp1b^{-/-}$ mice (n=8) and (d) male CON $Ptp1b^{fl/fl}$ (n=5), MR $Ptp1b^{fl/fl}$ (n=5) and MR $Alb\text{-}Ptp1b^{-/-}$ mice (n=5). Fasting serum triacylglycerol levels were measured in (e) female CON $Ptp1b^{fl/fl}$ (n=8), MR $Ptp1b^{fl/fl}$ (n=8) and MR $Alb\text{-}Ptp1b^{-/-}$ mice (n=8) and (f) male CON Ptp1b^{fl/fl} (n=5), MR $Ptp1b^{fl/fl}$ (n=5) and MR $Alb\text{-}Ptp1b^{-/-}$ mice (n=5). Hepatic gene expression in female CON $Ptp1b^{fl/fl}$ (n=5), MR $Ptp1b^{fl/fl}$ (n=4) and MR $Alb\text{-}Ptp1b^{-/-}$ mice (n=6).). Data are represented as mean ± s.e.m. White bars, CON $Ptp1b^{fl/fl}$; grey bars, MR $Ptp1b^{fl/fl}$; black bars, MR $Alb\text{-}Ptp1b^{-/-}$. Data were analysed by one-way ANOVA with Tukey's multiple comparison

post hoc test.* MR *Alb-Ptp1b*^{-/-} and MR *Ptp1b*^{fl/fl} mice significantly different to CON *Ptp1b*^{fl/fl} mice ($p < 0.05$).
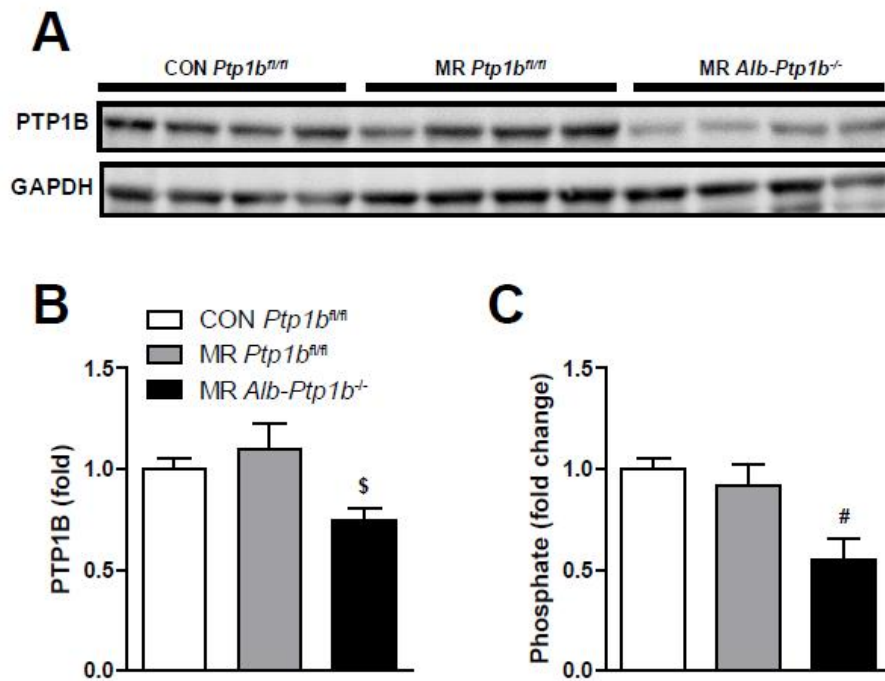
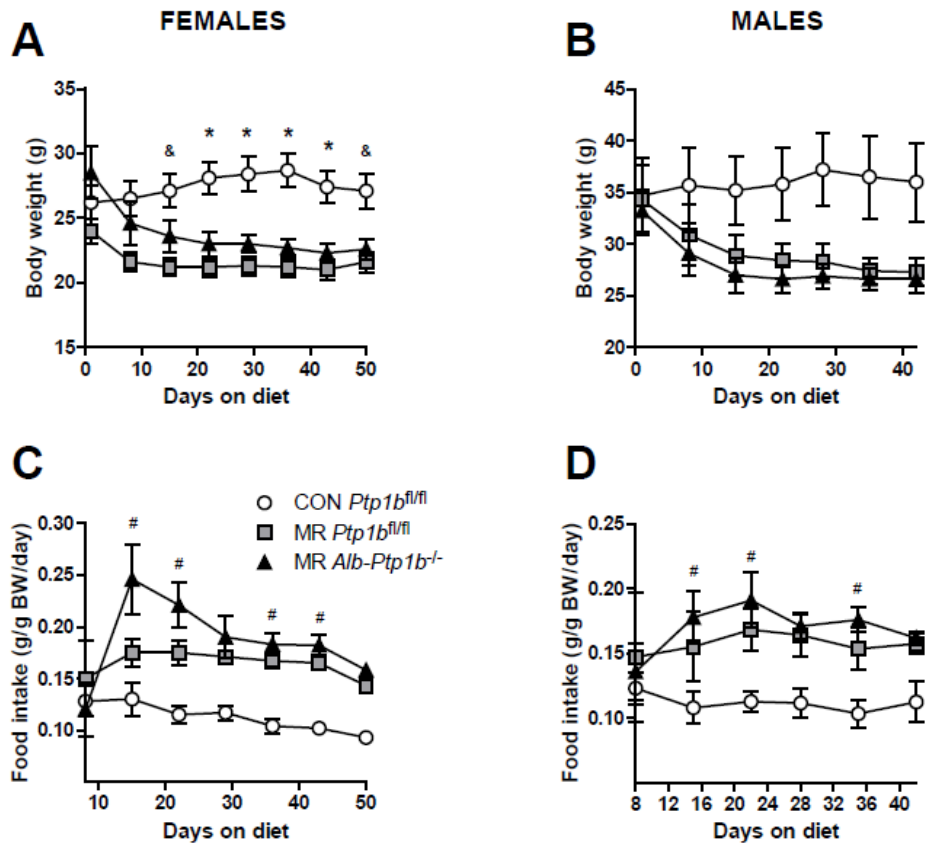**Fig. 1**

Fig. 2

A FEMALES

B MALES

C

CON $Ptp1b^{fl/fl}$
MR $Ptp1b^{fl/fl}$
MR $Alb-Ptp1b^{-/-}$

D

Fig. 3

Fig. 4

Fig. 5

FEMALES

MALES

A — Serum leptin (nmol/l)
- CON *Ptp1b*^fl/fl
- MR *Ptp1b*^fl/fl
- MR *Alb-Ptp1b*^-/-

B — Serum leptin (nmol/l)
- CON *Ptp1b*^fl/
- MR *Ptp1b*^fl/fl
- MR *Alb-Ptp1*

C — Serum NEFA (mmol/l)

D — Serum NEFA (mmol/l)

E — Serum triacylglycerol (mmol/l)

F — Serum triacylglycerol (mmol/l)

G — Relative gene expression
SREBP1A, SREBP1C, FAS, G6P, PEPCK